

# Luminescent Properties of $\text{Tm}^{3+}$ -doped $\text{BaY}_2\text{ZnO}_5$ Phosphors Prepared by Sol–Gel Method with Different Urea Concentrations

Hao-Long Chen,<sup>1</sup> Lay-Gaik Teoh,<sup>1</sup> Sean Wu,<sup>2</sup>  
Yi-Hong Cheng<sup>3</sup>, and Yee-Shin Chang<sup>3\*</sup>

<sup>1</sup>Department of Mechanical Engineering, National Pingtung University of Science and Technology,  
No. 1, Shuefu Road, Neipu, Pingtung 912, Taiwan

<sup>2</sup>Department of Chemical and Materials Engineering, Lунghwa University of Science and Technology,  
No. 300, Sec. 1, Wanshou Rd., Guishan, Taoyuan 333, Taiwan

<sup>3</sup>Department of Electronic Engineering, National Formosa University,  
No. 64, Wunhua Rd., Huwei, Yunlin 632, Taiwan

(Received January 7, 2023; accepted May 15, 2023)

**Keywords:** phosphors, thulium ions, urea, luminescent properties

Photoluminescence-based nanomaterial sensors doped with rare-earth elements have a potential for use in sensitive, portable, and low-cost detectors. The oxide with the formula  $\text{XY}_2\text{ZO}_5$  has potential for fluorescence applications because of its orthorhombic structure, stable physical and chemical properties, and high thermal stability. In this study,  $\text{BaY}_2\text{ZnO}_5$  phosphors with various concentrations of  $\text{Tm}^{3+}$  and urea ions were synthesized at 1200 °C for 8 h in air by the sol-gel method. The characteristics of the phosphor powders were analyzed by field-emission scanning electron microscopy, X-ray diffraction (XRD), and photoluminescence spectroscopy. The diffraction peaks of phosphors with  $\text{Tm}^{3+}$  ion doping concentrations from 0 to 5 mol% and urea additions from 1 to 50 wt% are attributed to the orthorhombic  $\text{BaY}_2\text{ZnO}_5$  structure examined by XRD analysis. When the  $\text{Tm}^{3+}$  ion concentration is 2 mol%, the maximum emission intensity of the  $^1\text{D}_2 \rightarrow ^3\text{F}_4$  transition can be obtained, which then decreases with increasing  $\text{Tm}^{3+}$  ion concentration. Concentration quenching occurs when the  $\text{Tm}^{3+}$  ion concentration is above 2 mol%. For  $\text{BaY}_2\text{ZnO}_5$  phosphors prepared by doping with  $\text{Tm}^{3+}$  ions and adding urea, excitation with an emission wavelength of 457 nm yields the color tone in the vivid blue region.

## 1. Introduction

Sensors have been widely used in various fields, such as machinery, electronics, and medical, optical, and chemical industries. The important requirements of sensors are stability, sensitivity, and selectivity, which are termed 3 ‘S’.<sup>(1)</sup> Owing to environmental changes and abnormal weather, the use of temperature, gas, and environmental monitoring sensors has gradually become widespread, and the need for stable sensing materials has been increasing. Photoluminescence-based nanomaterial sensors are currently the most promising candidates to

---

\*Corresponding author: e-mail: [yeeshin@nfu.edu.tw](mailto:yeeshin@nfu.edu.tw)  
<https://doi.org/10.18494/SAM4303>

resolve this issue because of their reliability, easy manufacturing, and various application fields.<sup>(2–5)</sup> Photoluminescence-based nanomaterials can be used for thermometry sensors, and lanthanide (La)-doped photoluminescent materials have advantages such as high chemical stability, narrow emission peaks, long emission decay lifetimes, temperature sensitivity, and low toxicity, which are promising for a new generation of potential applications.<sup>(5)</sup> The oxide with the formula  $XY_2ZO_5$  has been recognized as the most efficient host in fluorescence applications owing to its orthogonal structure, stable physicochemical properties, and high thermal stability.<sup>(5–8)</sup>

Rare-earth-ion-doped materials have attracted considerable attention because of their excellent photoluminescence properties.<sup>(9)</sup> Rare-earth ions in phosphors act as activators with f–f transitions that confine emission to the visible range for high efficiency and lumen-equivalent properties. Various  $Tm^{3+}$  ion-doped oxide host materials such as  $YVO_4:Tm^{3+}$ ,  $GdVO_4:Tm^{3+}$ , and  $YInGe_2O_5:Tm^{3+}$  phosphors producing a blue emission with excellent color coordinates have been extensively studied because they are stable with appropriate lifetimes and color-rendering properties under high-density excitation.<sup>(9,10)</sup>

$BaY_2ZnO_5$  has a stable orthorhombic crystal structure and high thermal stability, and its space group is Pbnm, which is an excellent photoluminescent host material.<sup>(11,12)</sup> The unit cell of  $BaY_2ZnO_5$  is composed of  $BaO_{11}$ ,  $YO_7$ , and  $ZnO_5$  polyhedra.

A given activator center in different host lattices exhibits various optical properties, which are attributable to activator center surroundings changed by a  $Tm^{3+}$  ion-doped phosphor. In this study,  $BaY_2ZnO_5$  phosphors with various concentrations of  $Tm^{3+}$  ions and urea were synthesized at 1200 °C for 8 h in air by the sol-gel method. The crystal structure and photoluminescence properties were then investigated.

## 2. Materials and Methods

$Tm^{3+}$  ion doping in  $BaY_2ZnO_5$ , formulated as  $Ba(Y_{1-x}Tm_x)_2ZnO_5$ , with  $x$  equal to 0–0.05 was performed by the sol-gel method. The raw materials used with purities of 99.99% were barium nitrate ( $BaNO_3$ ), zinc acetate ( $C_4H_{10}O_6Zn$ ), yttrium acetate [ $Y(OOCCH_3)_3$ ], thulium (III) nitrate [ $Tm(NO_3)_3$ ], and urea ( $CN_2H_4O$ ), which were purchased from Aldrich and Alfa Aesar Company. The doses of all starting materials were weighed stoichiometrically, and all the materials were dissolved separately in deionized water and mixed in a beaker with continuous stirring and dissolution at 50 °C for 5 h. The precursor was dissolved completely in the solution and then put in a furnace to dry at 50 °C for 4 days. After drying, the powders of the precursor were calcined at 1200 °C for 8 h using a programmable furnace.

The phases of the powders were identified using an X-ray powder diffractometer (Bruker AXS GmbH, D8 Advance, Germany), which uses Cu K $\alpha$  radiation with a source power of 30 kV and a current of 20 mA. The surface morphologies of the phosphors were observed with a field emission scanning electron microscope (Hitachi S4800-I, Japan). The absorption spectra of the phosphors were measured using a Hitachi U-3010 UV-visible spectrophotometer. The photoluminescence properties of the phosphors, including excitation and emission behaviors, were measured with a Hitachi F-7000 fluorescence spectrophotometer that uses a 150 W xenon

arc lamp as the excitation source. The absorption and photoluminescence properties were measured at room temperature.

### 3. Results and Discussion

The X-ray diffraction (XRD) results of  $\text{Ba}(\text{Y}_{1-x}\text{Tm}_x)_2\text{ZnO}_5$  ( $x = 0-0.05$ ) and  $\text{Ba}(\text{Y}_{0.98}\text{Tm}_{0.02})_2\text{ZnO}_5$  phosphors added with different urea concentrations and calcined at 1200 °C for 8 h in air are shown in Figs. 1(a) and 1(b), respectively. These results indicate that most of the diffraction peaks of the samples doped with different concentrations of  $\text{Tm}^{3+}$  ions and added with various urea concentrations were consistent with the orthorhombic structure of  $\text{BaY}_2\text{ZnO}_5$  (JCPDS No:89-5856). The properties of yttrium and other rare-earth ions are similar; thus, rare-earth ions can easily replace yttrium ions.<sup>(13)</sup> Kaduk *et al.* found that the crystal structures of  $\text{BaY}_2\text{ZnO}_5$  and  $\text{BaTm}_2\text{ZnO}_5$ , which were calculated by the Rietveld refinement method,<sup>(14)</sup> have the same space group as Pbnm. These results suggest that  $\text{Tm}^{3+}$  ions can be introduced to completely replace  $\text{Y}^{3+}$  ions in the  $\text{BaY}_2\text{ZnO}_5$  lattice and form solid solutions.<sup>(15)</sup> This is because  $\text{Tm}^{3+}$  (0.88 Å) and  $\text{Y}^{3+}$  (0.90 Å) ions have similar ionic radii. Both ions have the same valence, and in the  $\text{Ba}(\text{Y}_{1-x}\text{Tm}_x)_2\text{ZnO}_5$  system, when the  $\text{Y}^{3+}$  ion is replaced by the  $\text{Tm}^{3+}$  ion, the charge compensation problem does not occur.<sup>(16)</sup>

The SEM images of  $\text{Ba}(\text{Y}_{1-x}\text{Tm}_x)_2\text{ZnO}_5$  ( $x = 0.005-0.05$ ) phosphors are shown in Fig. 2. Figure 3 shows the SEM images of  $\text{Ba}(\text{Y}_{0.98}\text{Tm}_{0.02})_2\text{ZnO}_5$  phosphors added with different concentrations of urea and calcined at 1200 °C for 8 h. The SEM images show particle sizes of approximately 40–50 nm. Regardless of whether only  $\text{Tm}^{3+}$  ions were doped or different urea concentrations were added, the morphology of the particles was irregular and particle agglomeration occurred in the host system. The agglomeration is due to the small particles and the strong cohesion of phosphors prepared by the sol-gel method. The SEM images in Figs. 2 and 3 showed no significant differences; thus, the doping of  $\text{Tm}^{3+}$  ions or the addition of urea at different concentrations had no effect on the surface morphology of the  $\text{BaY}_2\text{ZnO}_5$  host.

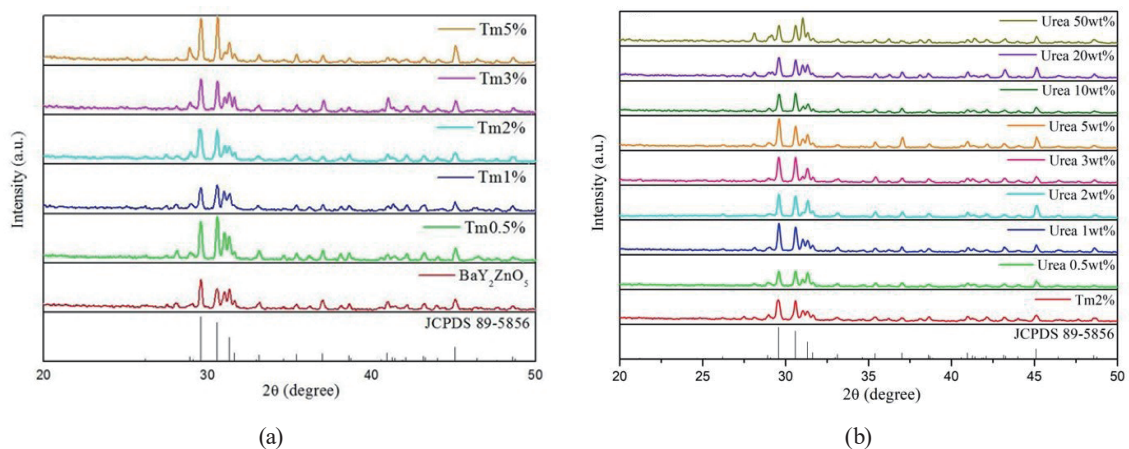


Fig. 1. (Color online) XRD results of (a)  $\text{Ba}(\text{Y}_{1-x}\text{Tm}_x)_2\text{ZnO}_5$  and (b)  $\text{Ba}(\text{Y}_{0.98}\text{Tm}_{0.02})_2\text{ZnO}_5$  phosphors added with different urea concentrations and calcined at 1200 °C for 8 h.

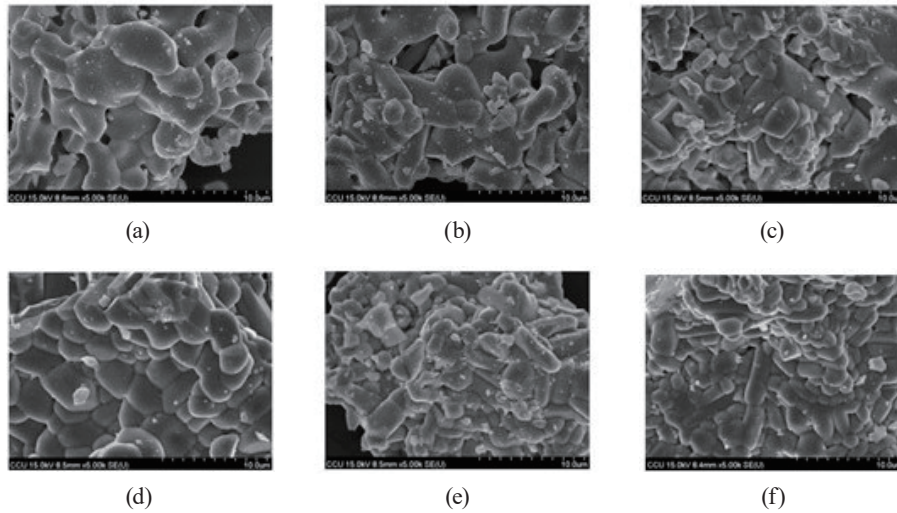


Fig. 2. SEM images of  $\text{Ba}(\text{Y}_{1-x}\text{Tm}_x)_2\text{ZnO}_5$  phosphors: (a)  $\text{BaY}_2\text{ZnO}_5$ , (b) Tm 0.5%, (c) Tm 1%, (d) Tm 2%, (e) Tm 3%, and (f) Tm 5%.

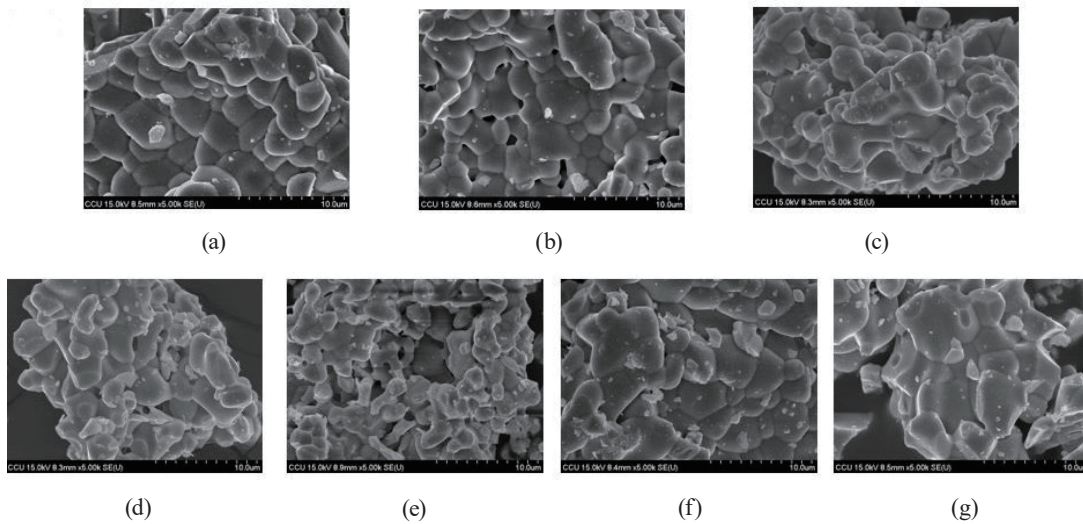


Fig. 3. SEM images of  $\text{Ba}(\text{Y}_{0.98}\text{Tm}_{0.02})_2\text{ZnO}_5$  phosphors added with different urea concentrations: (a) 0, (b) 1, (c) 3, (d) 5, (e) 10, (f) 20, and (g) 50 wt%.

The absorption spectra of  $\text{BaY}_2\text{ZnO}_5$  doped with different concentrations of  $\text{Tm}^{3+}$  ions and  $\text{Ba}(\text{Y}_{0.98}\text{Tm}_{0.02})_2\text{ZnO}_5$  added with different concentrations of urea ions, then calcined at  $1200\text{ }^\circ\text{C}$  for 8 h in air, are shown in Figs. 4(a) and 4(b), respectively. The results show a strong absorption appearance in the region from 200 to 250 nm, which is attributed to the band-to-band transitions of the  $\text{BaY}_2\text{ZnO}_5$  host.<sup>(13)</sup> The region from 270 to 400 nm has a weak broad peak that is attributed to the tightly bound Frankel excitons, which are usually observed near the band gap with a large band gap in crystals.<sup>(17)</sup> When  $\text{BaY}_2\text{ZnO}_5$  is doped with  $\text{Tm}^{3+}$  ions or added with different concentrations of urea ions, a group of sharp peaks appear at wavelengths of 362, 464, and 694 nm, which are assigned to the typical  $4f^n \rightarrow 4f^{n-1}5d$  intra-configuration forbidden transition for  $\text{Tm}^{3+}$  ions.<sup>(18)</sup> With increasing urea ion concentration, the absorption band between 350 and 750 nm is

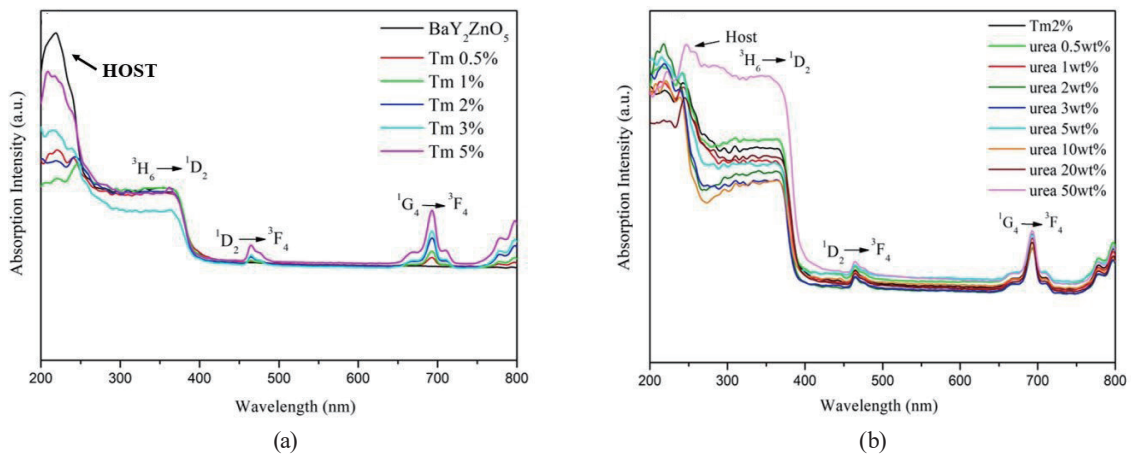


Fig. 4. (Color online) Absorption spectra of (a)  $\text{BaY}_2\text{ZnO}_5$  doped with different concentrations of  $\text{Tm}^{3+}$  ions and (b)  $\text{Ba}(\text{Y}_{0.98}\text{Tm}_{0.02})_2\text{ZnO}_5$  added with different concentrations of urea ions and calcined at  $1200^\circ\text{C}$  for 8 h.

not significantly enhanced. If the urea ion concentration is increased to 50 wt%, the main absorption peak at 250–380 nm will be significantly enhanced.

The PL excitation spectra of  $\text{BaY}_2\text{ZnO}_5$  doped with different concentrations of  $\text{Tm}^{3+}$  ions and  $\text{Ba}(\text{Y}_{0.98}\text{Tm}_{0.02})_2\text{ZnO}_5$  added with different concentrations of urea ions and calcined at  $1200^\circ\text{C}$  for 8 h in air are shown in Figs. 5(a) and 5(b), respectively. The excitation spectra were detected using the emission wavelength of 457 nm. The excitation spectrum wavelength range between 200 and 400 nm can be observed. The center of the broadband at 244 nm is classified as the band-to-band transition for the  $\text{BaY}_2\text{ZnO}_5$  host.<sup>(19)</sup> In addition, the two peaks that appear between 250 and 300 nm correspond to the  $\text{Tm}^{3+}$  ion  $4f^n \rightarrow 4f^n$  intra-configuration transition for  ${}^3\text{H}_6 \rightarrow {}^3\text{P}_0$  and  ${}^3\text{H}_6 \rightarrow {}^3\text{P}_2$ , and the strongest peak at 365 nm corresponds to the  ${}^3\text{H}_6 \rightarrow {}^1\text{D}_2$  transition.<sup>(20)</sup> When the doping concentration of the  $\text{Tm}^{3+}$  ion is 2 mol%, the excitation energy band in this region is at the maximum, and then it decreases as the doping concentration increases. It can be observed from Fig. 5(b) that the excitation peak is not shifted by adding urea ions. When the concentration of urea ions is 1 wt%, the excitation energy band at 365 nm is at the maximum, and then, it decreases as the urea ion concentration increases. Therefore, from the overall results, if  $\text{Tm}^{3+}$  ions are doped at 2 mol% and 1 wt% urea ions are added, the best excitation peak intensity will be obtained.

An excitation wavelength of 365 nm was used to excite  $\text{BaY}_2\text{ZnO}_5$  doped with different concentrations of  $\text{Tm}^{3+}$  ions and  $\text{Ba}(\text{Y}_{0.98}\text{Tm}_{0.02})_2\text{ZnO}_5$  added with various concentrations of urea ions, and their emission spectra are shown in Fig. 6. The main emission peaks at 457 nm are due to the  ${}^1\text{D}_2 \rightarrow {}^3\text{F}_4$  transitions of the  $\text{Tm}^{3+}$  ions.<sup>(20)</sup> There are also some very weak peaks at 480, 517, 666, and 735 nm, which correspond to the  ${}^1\text{G}_4 \rightarrow {}^3\text{H}_6$ ,  ${}^1\text{D}_2 \rightarrow {}^3\text{H}_5$ ,  ${}^1\text{G}_4 \rightarrow {}^3\text{F}_4$ , and  ${}^1\text{G}_4 \rightarrow {}^3\text{F}_5$  transitions, respectively. According to the literature, the rare-earth  $\text{Tm}^{3+}$  ion has three emission levels:  ${}^3\text{P}_0$  ( $35,000\text{ cm}^{-1}$ ),  ${}^1\text{D}_2$  ( $27,770\text{ cm}^{-1}$ ), and  ${}^1\text{G}_4$  ( $21,200\text{ cm}^{-1}$ ).<sup>(21)</sup> In  $\text{BaY}_2\text{ZnO}_5:\text{Tm}$  phosphors, it is enough to populate only the  ${}^1\text{D}_2$  ( $27,770\text{ cm}^{-1}$ ) or  ${}^1\text{G}_4$  ( $21,200\text{ cm}^{-1}$ ) emission level because the excited energy level is from the  ${}^3\text{H}_6 \rightarrow {}^1\text{D}_2$  transition of the  $\text{Tm}^{3+}$  ion itself.<sup>(20,22)</sup> It can be observed from Fig. 6(a) that the emission intensity increases and then decreases with

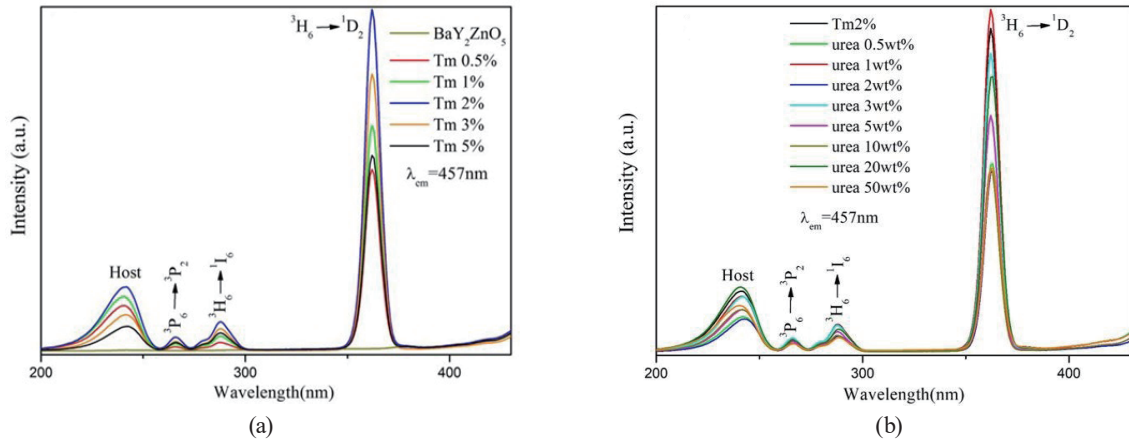


Fig. 5. (Color online) PL excitation spectra of (a)  $\text{BaY}_2\text{ZnO}_5$  doped with different concentrations of  $\text{Tm}^{3+}$  ions and (b)  $\text{Ba}(\text{Y}_{0.98}\text{Tm}_{0.02})_2\text{ZnO}_5$  added with different concentrations of urea ions and calcined at  $1200^\circ\text{C}$  for 8 h.

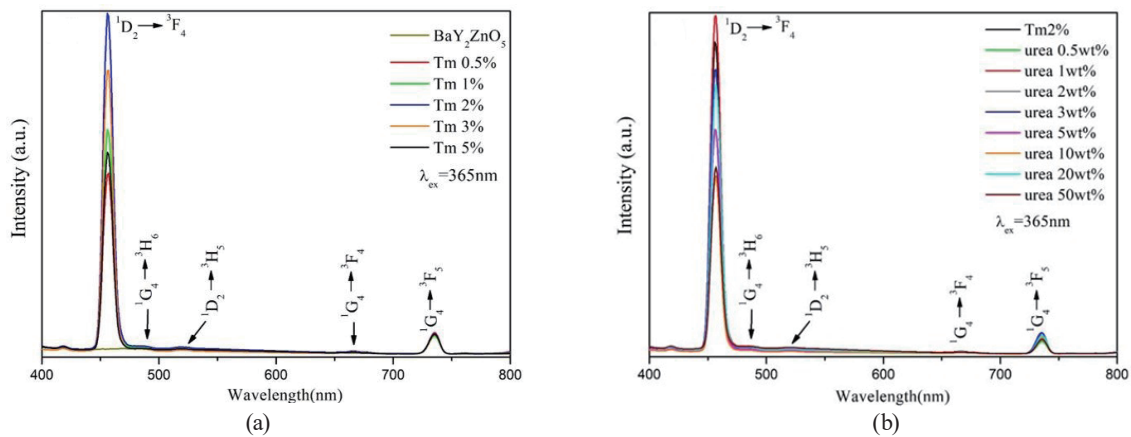


Fig. 6. (Color online) Photoluminescence emission spectra of (a)  $\text{BaY}_2\text{ZnO}_5$  doped with different concentrations of  $\text{Tm}^{3+}$  ions and (b)  $\text{Ba}(\text{Y}_{0.98}\text{Tm}_{0.02})_2\text{ZnO}_5$  added with different concentrations of urea ions under an excitation wavelength of 365 nm.

increasing  $\text{Tm}^{3+}$  ion concentration, with the maximum intensity being obtained at a  $\text{Tm}^{3+}$  ion concentration of 2 mol%. This is due to the concentration quenching effect in the rare-earth-ion-doped system.<sup>(21–24)</sup> Figure 6(b) shows that when the optimal doping concentration of  $\text{Tm}^{3+}$  ions is 2 mol%, the addition of low-concentration urea ions can enhance the main emission peak and the optimal value is 1 wt%. Then, the emission intensity is expected to decrease as the urea ion concentration increases. Therefore, from the overall results, if  $\text{Tm}^{3+}$  ions are doped at 2 mol% and 1 wt% urea ions are added, the best emission peak intensity will be obtained.

Figure 7 shows the Commission Internationale de l’Eclairage (CIE) chromaticity coordinates of  $\text{BaY}_2\text{ZnO}_5$  doped with different concentrations of  $\text{Tm}^{3+}$  ions [Fig. 7(a)] and  $\text{Ba}(\text{Y}_{0.98}\text{Tm}_{0.02})_2\text{ZnO}_5$  added with different concentrations of urea ions [Fig. 7(b)] under an excitation wavelength of 365 nm. For the  $\text{BaY}_2\text{ZnO}_5:\text{Tm}^{3+}$  phosphor, doping with different

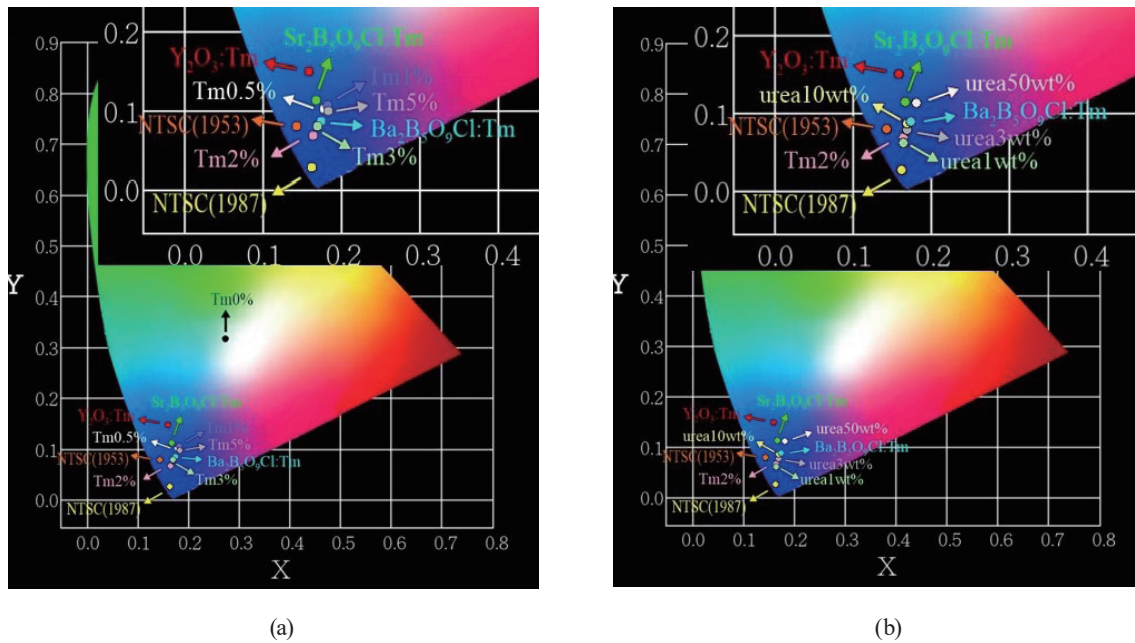


Fig. 7. (Color online) CIE chromaticity coordinates of (a)  $\text{BaY}_2\text{ZnO}_5$  doped with different concentrations of  $\text{Tm}^{3+}$  ions and (b)  $\text{Ba}(\text{Y}_{0.98}\text{Tm}_{0.02})_2\text{ZnO}_5$  added with different concentrations of urea ions.

concentrations of  $\text{Tm}^{3+}$  ions or adding different concentrations of urea ions has no effect on the shape of the emission curve, but the emission spectrum intensity is different. It can be seen in Fig. 7(a) that as the  $\text{Tm}^{3+}$  ion doping concentration increases, the CIE chromaticity coordinates change from the blue-green light region to the blue light region. The best  $\text{Tm}^{3+}$  concentration located in the blue light region is 2 mol%, and the chromaticity coordinates are ( $x = 0.164$ ,  $y = 0.07$ ). Figure 7(b) shows that when the optimal doping concentration of  $\text{Tm}^{3+}$  ions is 2 mol%, the addition of 1 wt% urea ions can enhance the luminous intensity of blue light. Its chromaticity coordinates are ( $x = 0.162$ ,  $y = 0.067$ ). The results show that the  $\text{BaY}_2\text{ZnO}_5$  phosphor doped with  $\text{Tm}^{3+}$  ions and added with a low concentration of urea ions emits a vivid blue light.

The PL properties of  $\text{Tm}^{3+}$  are strongly affected by not only its surroundings but also the blue emission intensity ratio and the energy transfer behavior between the  $\text{Tm}^{3+}$  concentration-dependent PL intensity and the chromaticity coordinates.<sup>(25)</sup> This result is also shown in Fig. 7.

## 5. Conclusions

Lanthanide-doped  $\text{BaY}_2\text{ZnO}_5$  phosphors are promising candidates for luminescence temperature thermometry applications. In this study, the  $\text{BaY}_2\text{ZnO}_5$  phosphor doped with  $\text{Tm}^{3+}$  and urea ions was successfully synthesized by the sol-gel method, and its luminescence region was blue light. The results of XRD analysis showed that all the samples doped with different concentrations of  $\text{Tm}^{3+}$  and urea ions were consistent with the orthorhombic structure of  $\text{BaY}_2\text{ZnO}_5$ . Regardless of whether only  $\text{Tm}^{3+}$  ions were doped or different concentrations of urea ions were added, the morphology of the particles was irregular and particle agglomeration

occurred in the host system. The agglomeration occurred because the phosphor powder prepared by the sol-gel method has strong cohesion. An excitation wavelength of 365 nm was used to excite BaY<sub>2</sub>ZnO<sub>5</sub>, and the main emission bands obtained at 457 nm are due to the <sup>1</sup>D<sub>2</sub>→<sup>3</sup>F<sub>4</sub> transitions of the Tm<sup>3+</sup> ions. There are also some very weak peaks at 480, 517, 666, and 735 nm, which correspond to the <sup>1</sup>G<sub>4</sub>→<sup>3</sup>H<sub>6</sub>, <sup>1</sup>D<sub>2</sub>→<sup>3</sup>H<sub>5</sub>, <sup>1</sup>G<sub>4</sub>→<sup>3</sup>F<sub>4</sub>, and <sup>1</sup>G<sub>4</sub>→<sup>3</sup>F<sub>5</sub> transitions, respectively. When the doping concentration of Tm<sup>3+</sup> ions is 2 mol% and that of urea ions is 1 wt%, the CIE chromaticity coordinates are (0.162, 0.067) in the vivid blue region.

### Acknowledgments

We would like to thank the Ministry of Science and Technology of the Republic of China for funding our study (project number MOST 107-2622-E-150-005-CC3).

### References

- 1 X. J. Huang and Y. K. Choi: *Sens. Actuators, B* **122** (2007) 659. <https://doi.org/10.1016/j.snb.2006.06.022>
- 2 H. H. Zhu, X. Y. Huang, Y. Deng, H. Chen, M. Fan, and Z. J. Gong: *Trac-trend Anal. Chem.* **158** (2023) 116879. <https://doi.org/10.1016/j.trac.2022.116879>
- 3 R. V. Bovhyra, S. I. Mudry, D. I. Popovych, S. S. Savka, A. S. Serednytski, and Y. I. Venhryn: *Appl. Nanosci.* **9** (2019) 775. <https://doi.org/10.1007/s13204-018-0697-9>
- 4 S. E. Crawford, P. R. Ohodnicki Jr., and J. P. Baltrus: *J. Mater. Chem. C* (2020). <https://doi.org/10.1039/D0TC01939A>
- 5 X. Y. Li, X. T. Wei, Y. U. Qin, Y. G. Chen, C. K. Duan, and M. Yin: *J. Alloys Comp.* **657** (2016) 353. <https://doi.org/10.1016/j.jallcom.2015.10.101>
- 6 L. Li, C. Guo, S. Jiang, D. K. Agrawal, and T. Li: *RCS Adv.* **4** (2014) 6391. <https://doi.org/10.1039/C3RA47264G>
- 7 I. Etchart, M. Bérard, M. Laroche, A. Huignard, I. Hernández, W. P. Gillin, R. J. Curry, and A. K. Cheetham: *Chem. Commun.* **47** (2011) 6263. <https://doi.org/10.1039/C1CC11427A>
- 8 H. R. Shih, M. T. Tsai, L. G. Teoh, and Y. S. Chang: *J. Mod. Phys.* **10** (2019) 91. <https://doi.org/10.4236/jmp.2019.102008>
- 9 Y. Nakanishi, H. Wada, H. Kominami, M. Kottaisamy, T. Aoki, and Y. Hatanaka: *J. Electrochem. Soc.* **146** (1999) 4320. <https://doi.org/10.1149/1.1392634>
- 10 H. J. Lin and Y. S. Chang: *Electrochem. Solid State Lett.* **10** (2007) J79. <https://doi.org/10.1149/1.2732076>
- 11 X. Zhao, X. Wang, B. Chen, Q. Meng, W. Di, G. Ren, and Y. Yang: *J. Alloy. Compd.* **433** (2007) 352. <https://doi.org/10.1016/j.jallcom.2006.06.096>
- 12 Materials Project: DOE Data Explorer, Materials Data on BaY<sub>2</sub>ZnO<sub>5</sub>, <https://doi.org/10.17188/1277717> (accessed July 2020).
- 13 H. R. Shih and Y. S. Chang: *J. Electron. Mater.* **46** (2017) 6603. <https://doi.org/10.1007/s11664-017-5717-0>
- 14 J. A. Kaduk W. Wing-Ng, W. Greenwood, J. Dillingham, and B. H. Toby: *J. Res. Natl. Inst. Stand. Technol.* **104** (1999) 147. <https://doi.org/10.6028/jres.104.011>
- 15 S. Chahar, V. B. Taxak, M. Dalal, S. Singh, and S. P. Khatkar: *Mater. Res. Bull.* **77** (2016) 91. <https://doi.org/10.1016/j.materresbull.2016.01.027>
- 16 R. D. Shannon: *Acta Cryst.* **A32** (1976) 751. <https://doi.org/10.1107/s0567739476001551>
- 17 K. Hashizume, M. Matsubayashi, M. Vachal, and T. Tani: *J. Lumin.* **98** (2002) 49. [https://doi.org/10.1016/s0022-2313\(02\)00251-x](https://doi.org/10.1016/s0022-2313(02)00251-x)
- 18 G. Blasse and B. C. Grabmaier: *Luminescent Materials* (Springer, Berlin, 1994).
- 19 M. Dalala, V. B. Taxaka, S. Chahara, and J. Dalal: *J. Alloy. Compd.* **686** (2016) 366. <https://doi.org/10.1016/j.jallcom.2016.06.040>
- 20 O. A. Serra, E. J. Nassar, P. S. Calefi, and I. L. V. Rosa: *J. Alloys Compd.* **275–277** (1998) 838. [https://doi.org/10.1016/S0925-8388\(98\)00453-8](https://doi.org/10.1016/S0925-8388(98)00453-8)
- 21 Y. Zhang, S. Xu, X. Li, J. Sun, J. Zhang, H. Zheng, H. Zhong, R. Hua, H. Xia, and B. Chen: *J. Alloys Compd.* **709** (2017) 147. <https://doi.org/10.1016/j.jallcom.2017.03.125>

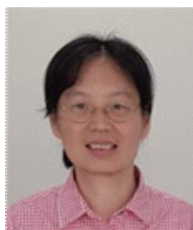


- 22 H. Lai, B. Chen, W. Xu, X. Wang, Y. Yang, and Q. Meng: J. Alloys Compd. **395** (2005) 181. <https://doi.org/10.1016/j.jallcom.2004.10.074>
- 23 M. Akatsuka, G. Okada, D. Nakauchi, T. Kato, N. Kawaguchi, and T. Yanagida: J. Lumin. **228** (2020) 117610. <https://doi.org/10.1016/j.jlumin.2020.117610>
- 24 P. Kantuptim, M. Akatsuka, D. Nakauchi, T. Kato, N. Kawaguchi, and T. Yanagida: J. Alloys Compd. **847** (2020) 156542. <https://doi.org/10.1016/j.jallcom.2020.156542>
- 25 H. Y. Zhang, B. S. Cao, Z. C. Liao, Y. W. Yang, J. Zhang, L. P. Li, Y. Cong, Y. Y. He, Z. Zhang, Z. Q. Feng, and B. Dong: Ceram. Int. **48** (2022) 29838. <https://doi.org/10.1016/j.ceramint.2022.06.248>

## About the Authors



**Hao-Long Chen** received his B.S. degree from National Taiwan Ocean University, Taiwan, in 1991, his M.S. degree from National Taiwan University of Science and Technology, Taiwan, in 1994, and his Ph.D. degree from National Cheng Kung University, Taiwan, in 2005. His research interests are in phosphor materials, sensor materials, energy materials, and nanomaterials. ([hlchern@ms18.hinet.net](mailto:hlchern@ms18.hinet.net))



**Lay Gaik Teoh** is a professor in the Department of Mechanical Engineering of National Pingtung University of Science and Technology, Pingtung, Taiwan. Her research interests include phosphor materials, dielectric materials, gas sensors, and nanomaterials. ([n5888107@gmail.com](mailto:n5888107@gmail.com))



**Sean Wu** received his B.S. degree in electrical engineering in 1993 from Chung Yuan Christian University in Taiwan, and his M.S. and Ph.D. degrees in electrical engineering from National Cheng Kung University in 1995 and 2001, respectively. He joined the Department of Electronics Engineering and Computer Science, Tung Fang Design University and became a professor in 2010. Since 2020, he has been a professor at Lunghwa University of Science and Technology. His research interests are in the fabrication of piezoelectric thin films, the design of acoustic wave devices, and substrate materials for SAW and FBAR devices. ([wusean.tw@gmail.com](mailto:wusean.tw@gmail.com))



**Yi-Hong Cheng** received his B.S. and M.S. degrees from National Formosa University, Taiwan, in 2016 and 2020, respectively. His research interests include phosphor materials, sensor materials, and nanomaterials. ([yeeshin@nfu.edu.tw](mailto:yeeshin@nfu.edu.tw))



**Yee-Shin Chang** received his M.S. and Ph.D. degrees from National Cheng Kung University, Taiwan, in 2000 and 2004, respectively. From 2004 to 2006, he was a principal engineer in United Microelectronics Corporation (UMC) in Taiwan. From 2006 to 2009, he was an assistant professor at National Formosa University, Taiwan. Since 2012, he has been a professor at National Formosa University. His research interests are in phosphor powder synthesis, dielectric ceramics, and electro-optic ceramics. ([yeeshin@nfu.edu.tw](mailto:yeeshin@nfu.edu.tw))